# Advance, Retreat, and Halt of Abrupt Gravel-Sand Transitions in Alluvial Rivers

Blom, Astrid; Chavarrias Borras, Victor; Ferguson, Robert I.; Viparelli, Enrica

**Important note**
To cite this publication, please use the final published version (if applicable).
Please check the document version above.

# Advance, Retreat, and Halt of Abrupt Gravel-Sand Transitions in Alluvial Rivers

**Astrid Blom**[1] [ID], **Víctor Chavarrías**[1] [ID], **Robert I. Ferguson**[2] [ID], **and Enrica Viparelli**[3] [ID]

[1]Faculty of Civil Engineering and Geosciences, Delft University of Technology, Delft, Netherlands, [2]Department of Geography, Durham University, Durham, UK, [3]Department of Civil and Environmental Engineering, University of South Carolina, Columbia, SC, USA

**Abstract** Downstream fining of bed sediment in alluvial rivers is usually gradual, but often an abrupt decrease in characteristic grain size occurs from about 10 to 1 mm, i.e., a gravel-sand transition (GST) or gravel front. Here we present an analytical model of GST migration that explicitly accounts for gravel and sand transport and deposition in the gravel reach, sea level change, subsidence, and delta progradation. The model shows that even a limited gravel supply to a sand bed reach induces progradation of a gravel wedge and predicts the circumstances required for the gravel front to advance, retreat, and halt. Predicted modern GST migration rates agree well with measured data at Allt Dubhaig and the Fraser River, and the model qualitatively captures the behavior of other documented gravel fronts. The analysis shows that sea level change, subsidence, and delta progradation have a significant impact on the GST position in lowland rivers.
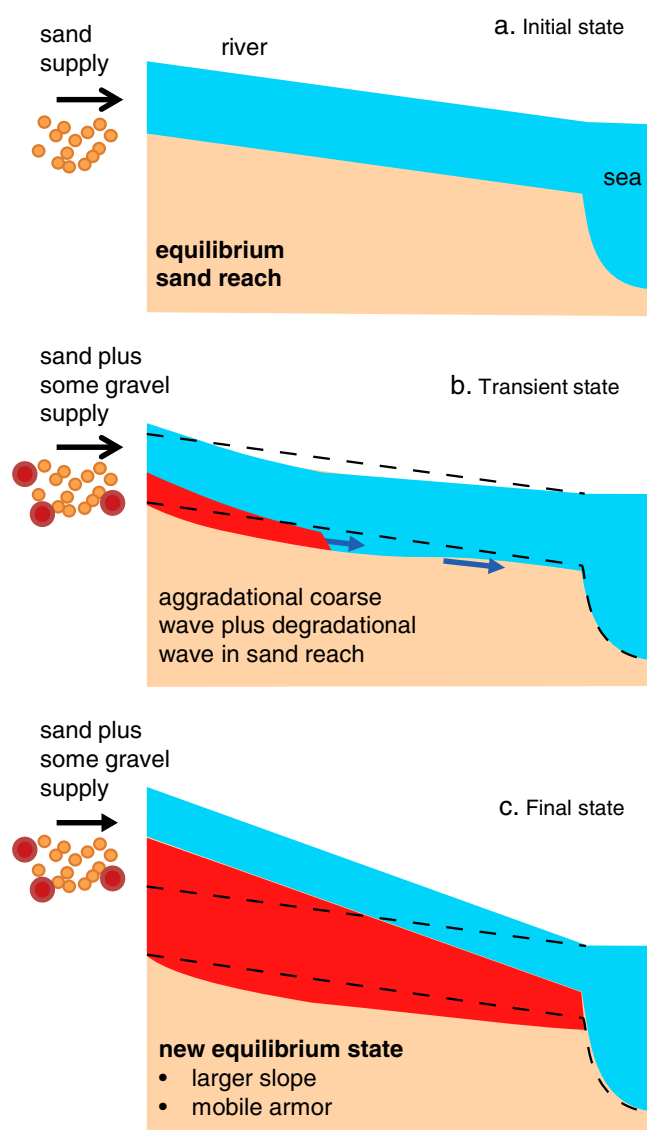
## 1. Introduction

Rivers are usually characterized by downstream fining of their bed surface sediment and a concave upward longitudinal profile (Blom et al., 2016; Sinha & Parker, 1996; Sternberg, 1875). A special case of the downstream decrease in surface grain size is the relatively abrupt transition from a gravel reach to a sand reach (gravel-sand transition, GST, Yatsu, 1955), which makes river reaches with a characteristic bed surface grain size in the 1–10 mm range rare (Jerolmack & Brzinski, 2010; Lamb & Venditti, 2016; Shaw & Kellerhals, 1982). A GST is generally accompanied by a similarly abrupt transition in channel slope. The correlation between bed grain size and channel slope arises from the fact that coarse sediment requires a larger shear stress and channel bed slope to be transported downstream than fine sediment (Blom et al., 2016; Howard, 1980; Mackin, 1948).

Suggested explanations for GST origin include preferential breakdown of 1–10 mm sized particles into sand (Yatsu, 1955); the load running out of gravel or progradation of a gravel front (Paola, Parker, et al., 1992; Parker & Cui 1998); downstream change in wash load transport (Lamb & Venditti, 2016; Parker, 2004; Venditti & Church, 2014); a threshold sand content above which a reach starts behaving as a sand reach (Wilcock, 1998); and the fact that fines are more mobile than coarse particles (i.e., grain size selectivity) (Ferguson, 2003; Ferguson et al., 2011; Jerolmack & Brzinski, 2010).

The bedload upstream from a GST usually has a bimodal size distribution (Wathen et al., 1995). This bimodality of the sediment supply is considered to be required for GST formation (Jerolmack & Brzinski, 2010; Parker & Cui, 1998) and originates from (a) bedrock weathering at the sediment source (Wolcott, 1988); (b) particle abrasion creating a discrete class of silt and fine sand (Jerolmack & Brzinski, 2010); and (c) the reduction of collision efficiency with reducing gravel size, which sets a lower limit of about 10 mm to gravel size (Jerolmack & Brzinski, 2010).

Despite the extent of studies, questions remain about how a GST forms, whether it migrates, if so at what speed, and if not where it halts. Our objectives are to describe the physics of GST migration and to develop a simple model of migration and halt of an abrupt GST. We assume sand to be part of the (suspended) bed material load and not wash load, where the latter is defined as the part of the load that does not directly affect channel slope, width, and main channel surface texture (Church, 2006; Paola, 2001). As the sand surface content is typically of the order of 10–20% (Litwin Miller et al., 2014; Parker et al., 1982), it affects the gravel load (Wilcock & Crowe, 2003) and channel slope.

sand
supply

river

a. Initial state

sea

**equilibrium
sand reach**

sand plus
some gravel
supply

b. Transient state

aggradational coarse
wave plus degradational
wave in sand reach

sand plus
some gravel
supply

c. Final state

**new equilibrium state**
*   larger slope
*   mobile armor

**Figure 1.** Formation of an abrupt GST due to gravel supply to a sand reach and development toward a new alluvial equilibrium state. Red areas indicate the gravel wedge and dashed lines indicate the initial state. Blue arrows indicate the aggradational and degrational waves. For simplicity the schematics do not account for the effects of particle abrasion (Blom et al., 2016).

## 2. The Physics of the GST

Our approach is to consider the consequences of adding a small amount of gravel to the sand supply to a graded or equilibrium sand bed reach (Figure 1). The gravel supply requires an increased slope to be transported downstream and thus a relatively steep gravel wedge forms through aggradation, which implies that the sediment flux decreases along the wedge. At the wedge front (i.e., at the position where the load runs out of gravel) an abrupt GST forms and slowly migrates downstream.

As the gravel reach lengthens, the sediment volume required for aggradation increases and consequently the wedge front decelerates. A GST can halt in systems governed by subsidence, delta progradation, or base level rise (Parker, 2004) due to the creation of accommodation space for the gravel supply in the gravel reach (Dingle et al., 2017; Marr et al., 2000; Paola, Heller, et al., 1992).

The large slope of the gravel reach makes sand so mobile that a small surface sand content suffices to transport the sand supply downstream, even though the bulk of the sediment flux can be in the sand size range (Leopold, 1992; Wilcock, 1998).

Although gravel can only pass the wedge front by building an increased slope, the sand and silt load experience no problem passing the front. Yet a fraction of the sand supply is trapped in the wedge deposit, as a deposit is generally formed out of transported and bed surface sediment (Hoey & Ferguson, 1994; Parker, 1991). As such, wedge formation reduces the sand supply to the sand reach and therefore the sand reach slope (Figure 1).

The two reaches have a different slope, and, as such, they are governed by a different flow depth: for a given water discharge and a spatially constant channel width the flow depth over the steep gravel reach is smaller than in the downstream sand reach. In the case of an abrupt transition this implies that the gravel front likely has a certain height (Figure 1). A GST may be less abrupt due to backwater effects, adaptation lengths of various parameters, and gravel overtaking the front such as at the Fraser River GST (Venditti et al., 2015).

## 3. The GST Migration Celerity

To derive an analytical GST migration model, we seek the simplest model capable of representing the essential physics (Paola & Leeder, 2011). Our simplifications are as follows: we consider a bimodal sediment supply that consists of gravel and sand, each represented by a single characteristic grain size; we neglect losses through abrasion; sand transport in the gravel reach depends on the bed surface sand content; spatial changes in slope within the gravel reach (e.g., concavity) are assumed to be small compared to the difference between the characteristic slopes of the two reaches; channel width, friction, bed porosity, and sediment density are constant; floodplains, tributaries, and bifurcations are not accounted for; we assume the GST to be abrupt; and we assume a characteristic flow rate (e.g., the channel-forming discharge, Blom et al., 2017), which may change with time.

We impose conservation of sediment mass within the gravel wedge (Figure 2). The gravel wedge volume changes if (1) the wedge front migrates; (2) the mean gravel reach slope changes; or (3) the elevation of the wedge front crest changes. Appendices A and B detail the derivation of the analytical model of GST migration. Assuming the temporal change of the reach slopes to generally be small, the average GST migration celerity, $c_A$, is given by

$$c_A = \frac{1}{\bar{S}_u - \bar{S}_d} \left[ \frac{Q_0}{c_b B} \frac{p_0}{\bar{F}_W} \frac{1}{x_A} - \xi - \bar{S}_d \beta + \omega \right] \qquad (1)$$
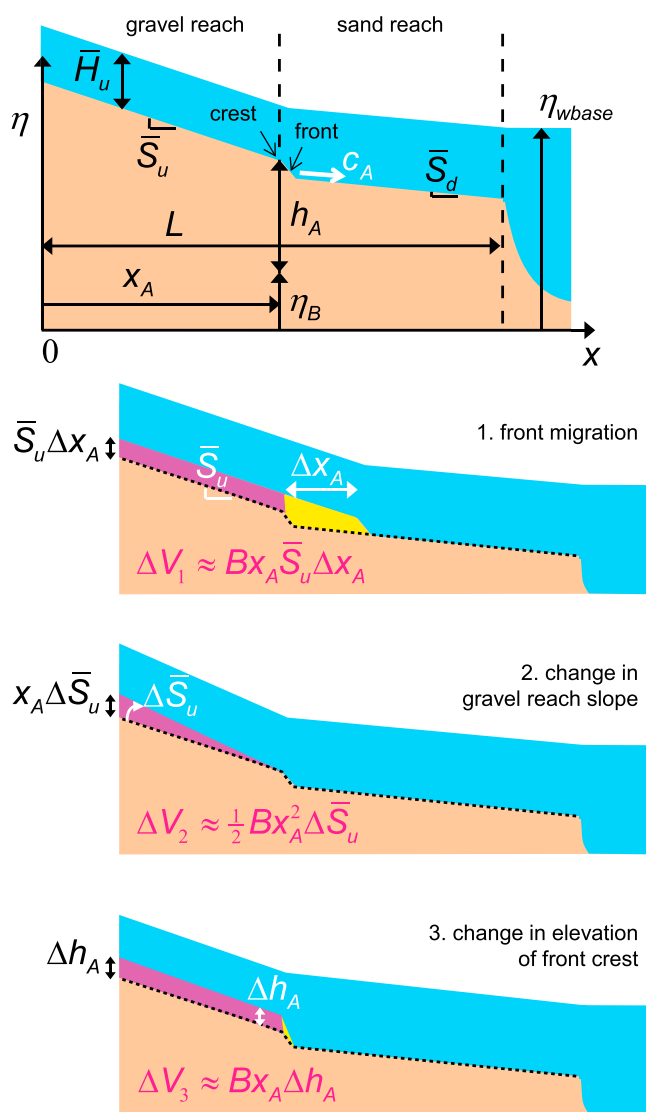
**Figure 2.** Parameter definitions and sources of change in gravel wedge volume. The sum of purple and yellow areas represents the change in gravel wedge volume related to either (1) wedge front migration; (2) change in mean gravel reach slope; or (3) change in elevation of the wedge front crest. Volume change associated with the yellow areas is neglected compared to the purple areas, which is reasonable if $x_A$ covers a significant distance.

where $\bar{S}_u$ and $\bar{S}_d$ denote the mean slopes of the gravel reach and sand reach, respectively, $Q_0$ the sediment supply rate at a certain position $x_0$ in the gravel wedge ($x_0 = 0$), $p_0$ the gravel content in the sediment supply ($0 < p_0 \leq 1$), $c_b$ the volumetric sediment concentration within the bed ($c_b = 1 - \lambda_p$ with $\lambda_p$ denoting bed porosity), $B$ the channel width, $\bar{F}_W$ the gravel content in the gravel reach subsurface ($0 < \bar{F}_W \leq 1$), $x_A$ the streamwise distance between the gravel front and position $x_0$, $\xi$ the rate of sea level rise, $\beta$ the delta progradation rate ($\beta = \mathrm{d}L/\mathrm{d}t$ with $L$ denoting the domain length), and $\omega$ is a uniform uplift rate. Equation (1) is a simplified version of equation (B1) in Appendix B. The GST migration celerity, $c_A$, in equation (1) is averaged over a period of many years or decades and over many floods of different magnitude.

## 4. The Stable GST

A GST halts when the migration celerity is zero ($c_A = 0$). We find that a stable GST position, $\tilde{x}_A$, exists provided that $\xi + \bar{S}_d \beta - \omega > 0$:

$$\tilde{x}_A = \frac{Q_0}{c_b B} \frac{p_0}{\bar{F}_W} \frac{1}{(\xi + \bar{S}_d \beta - \omega)} \quad (2)$$

which is essentially equivalent to the stable GST position derived in an earlier analysis by Parker (2004). Equation (2) illustrates that subsidence ($\omega < 0$), base level rise ($\xi > 0$), or delta progradation ($\beta > 0$) guarantee the existence of a stable GST position, $\tilde{x}_A$. A second condition for GST halt is the fact that the stable GST position is within the domain (i.e., $\tilde{x}_A < L$). If this is the case, the GST will naturally evolve toward the stable position (Parker, 2004), which is also nicely illustrated in laboratory experiments by Baumanis and Kim (2016). The Selenga River is an example where subsidence caused the GST to halt (Dong et al., 2016).

The GST continues to prograde if $\xi + \bar{S}_d \beta - \omega \leq 0$ or if the stable GST position is located downstream from the river mouth ($\tilde{x}_A \geq L$). In these cases the entire domain will eventually become gravel bedded. Examples are rivers in Japan, New Zealand, and the U.S. West Coast (Parker & Cui, 1998).

When the GST migration celerity, $c_A$, is negative, the GST retreats. This can result from upstream migration of a GST due to an increased rate of subsidence (Marr et al., 2000), base level rise, or delta progradation, as illustrated by equation (2).

The model illustrates that the characteristic flow rate affects GST migration and the stable GST position to a limited extent: it does so only through affecting the gravel reach and sand reach slopes. An increase of the characteristic flow rate reduces the gravel and sand reach slopes (Blom et al., 2016), which enhances GST advance (Marr et al., 2000) as the relative effect of the sand reach slope on GST migration is almost negligible compared to the gravel reach slope. If the stable GST position is known, equation (2) can aid in constraining the gravel flux (Dingle et al., 2017).

## 5. Extended Model

To compute the GST migration celerity with equation (1) or (B1), various parameters, among which the gravel flux, need to be specified. Closure relations for these parameters can be determined from (a) measured field data, possibly with the rarely available gravel flux estimated from measured values of slope and characteristic flow rate or (b) imposing a mean gravel flux and applying the approach described below.

Here we apply closure relations for slope and surface texture that are based on the assumption that both the gravel and the sand reach are in a state of quasi-equilibrium. We introduce the term "extended model" to
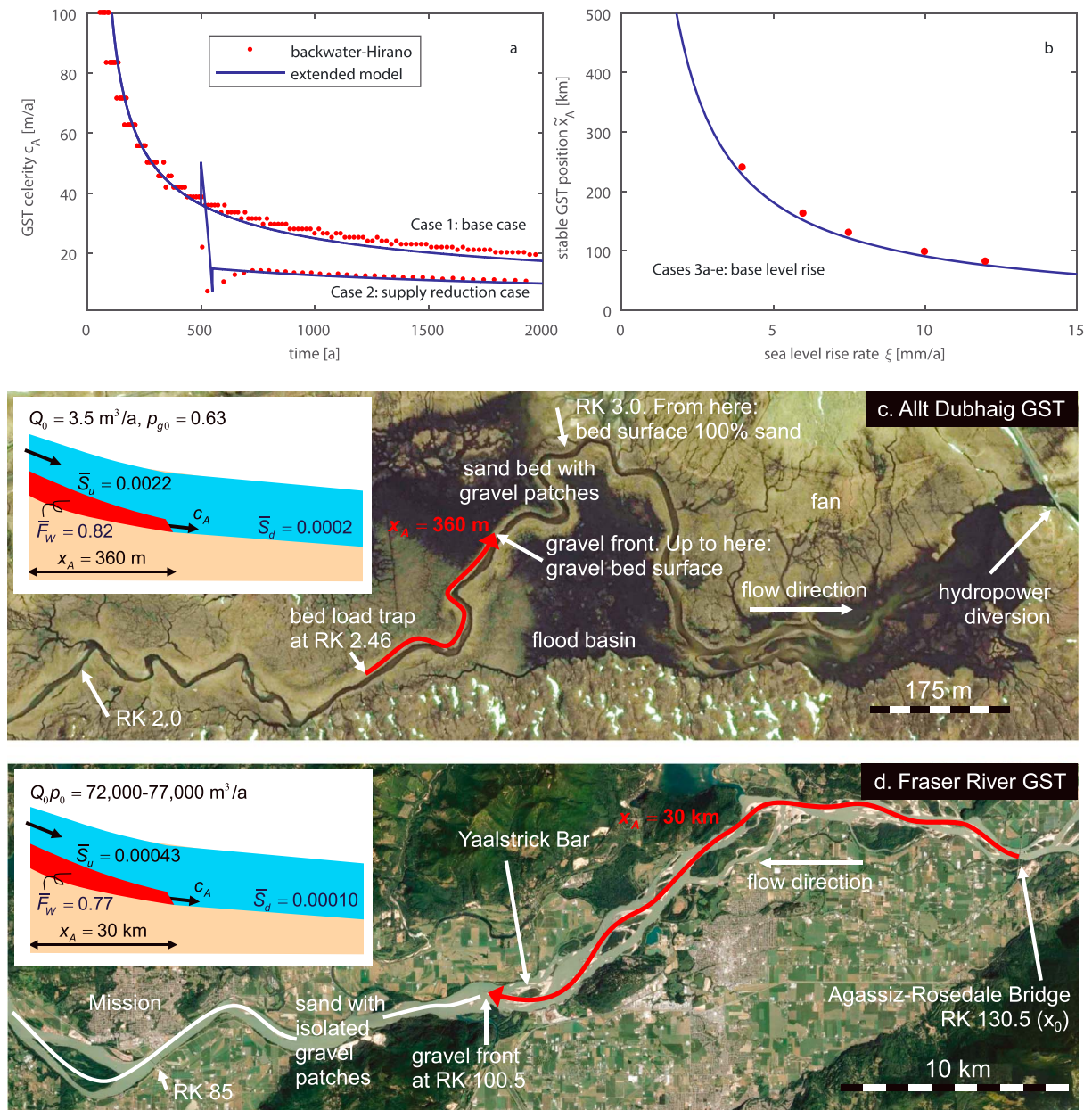
**Figure 3.** Application of the GST migration model. Validation of the extended model against the backwater-Hirano model illustrated by (a) the GST migration celerity, $c_A$, as a function of time for the base case and a supply reduction case (Case 2) in which after 500 years the gravel and sand supply rates decrease by 50% (the staircase effects in the backwater-Hirano model predictions result from its grid); and (b) the stable GST position, $\tilde{x}_A$, as a function of the rate of base level rise, $\xi$ (Cases 3a – 3e). Application of the GST migration model to two field cases: (c) the lower part of Allt Dubhaig in Scotland and (d) the Fraser River in Canada. The red lines indicate the distance $x_A$, which is the streamwise distance between position $x_0$ (where the gravel flux contributing to wedge progradation, $Q_0 p_0$, is known) and the gravel front.

indicate the combination of the analytical model of GST migration in equation (B1) and the quasi-equilibrium closure relations. The quasi-equilibrium state refers to the fact that, despite their transient state due to GST migration, the gravel reach and the sand reach are at grade with the water discharge and their gravel and sand supply rates. This assumption holds provided that boundary conditions change slowly (i.e., the time scale of the changing boundary conditions is larger than the time scale of channel response to the changing boundary conditions; Howard, 1982). Under these assumptions we can apply the formulations for slope and surface texture in an equilibrium alluvial reach derived by Blom et al. (2016) to the upstream ends of the gravel and sand reaches. The resulting values are assumed to represent reach-averaged values.

## 6. Validation of Extended Model

Our first test is the validation of the extended model against a more comprehensive numerical model based on conservation equations for mixed-size sediment (Hirano, 1971) and the backwater equation (Parker, 2004). The two models are applied to a base case in which rates of base level change, subsidence, and delta progradation are equal to zero. The sediment supply consists of 30% gravel, yet the initial conditions correspond to an equilibrium reach where the sediment supply consists of 100% sand. As such, the base case represents the schematic in Figure 1. Appendix C describes the remaining specifications.

The extended model predictions closely match those of the backwater-Hirano model (Figure 3a). As the gravel reach lengthens, the wedge front migrates at an ever slower pace. A decrease in sediment supply reduces the GST migration celerity, but (in the absence of subsidence, base level rise, or delta progradation) does not lead to GST retreat.

Base level rise leads to GST halt (Figure 3b). The faster the base level rises, the farther upstream the GST halts. The small difference between the backwater-Hirano model and the extended model predictions is because the latter assumes gravel reach-averaged values.

## 7. Allt Dubhaig and Fraser River

Our second test is the application of the analytical model of GST migration in equation (1) to estimate the modern GST migration celerities in Allt Dubhaig, Scotland, UK, and the much larger Fraser River, British Columbia, Canada. Both rivers drain areas of resistant igneous or metamorphic rocks, which implies that abrasion can be assumed negligible over the considered distances. In addition, in both rivers the GST migration rate is known over a period long enough for the effects of individual floods to average out. The GST position is defined as the location where the bed changes from a predominantly gravel bed surface into a predominantly sand bed surface, possibly with gravel patches.

Allt Dubhaig is a small headwater stream that flows along a glacial trough in the Scottish Highlands (Sambrook Smith & Ferguson, 1995; Wathen et al., 1995). Both the channel and valley floor are gravel dominated up to river kilometer (RK) 1.7 (i.e., 1.7 km downstream from where the stream leaves bedrock and enters the trough), but farther downstream a narrow gravel-dominated channel belt is surrounded by peat and fine floodplain deposits, suggesting that a gravel wedge has prograded along the channel during the Holocene (Ferguson et al., 1996, 1998). The gravel front was at RK 2.82 in 1991, and the bed consisted of entirely sand from RK 3.0 (Figure 3c) (Sambrook Smith & Ferguson, 1995). A low hydropower diversion dam built in the sand bed reach in 1935 backs water up less than 1 m. Coring along the GST in 1997 indicated that the gravel front retreated by about 80 m due to the dam's backwater effect and subsequently readvanced by about 50 m. This suggests a migration rate of about 0.8 m/a from the 1930s to the 1990s.

Data collected in 1991–1993 at a bedload trap at RK 2.46, 360 m upstream from the GST ($x_A = 360$ m), provide values of $Q_0$ (3.5 m³/a) and $p_0$ (0.63) (Wathen et al., 1995). With $\bar{S}_u = 0.0022$, $\bar{S}_d = 0.0002$ (Sambrook Smith & Ferguson, 1995), $B = 8$ m, $\bar{F}_W = 0.82$ (Wathen et al., 1995), $c_b = 0.7$, and negligible base level rise, subsidence, and delta progradation, the predicted GST celerity is 0.7 m/a, which agrees with the inferred advance since the 1930s.

The Fraser River is a largely unmodified river with a mean annual flood of 9,790 m³/s (McLean et al., 1999; Venditti & Church, 2014). Its GST is located in the lower alluvial reach at RK 100.5, which is 100.5 km upstream from the delta front and 15 km upstream from Mission (Figure 3d). Here part of the gravel load overtakes the gravel front and remains mobile in the upstream part of the sand reach (Venditti et al., 2015). The less than order of magnitude difference in slope over the front does not sufficiently reduce gravel mobility to trap all gravel load within the extended front. This seems to be a self-reinforcing effect as the gravel load overtaking the front contributes to steepening the upstream part of the sand reach, which reduces the slope difference between the two reaches even more.

Application of equation (1) requires the following input values: $\bar{S}_u = 0.00043$ and $\bar{S}_d = 0.00010$; $B = 925$ m; $\bar{F}_W$ is 0.77 (Venditti & Church, 2014); and $c_b$ is taken as 0.7. Sediment budget analyses over the period 1952–1999 reveal values for the gravel flux at Agassiz-Rosedale Bridge (30 km upstream from the GST) of 100,000–140,000 m³/a (Ham & Church, 2012; Venditti & Church 2014) as well as an increased gravel flux from 1999 up to at least 2003 due to erosion associated with channel alignment upstream of Agassiz-Rosedale

Bridge (Ham, 2005). Annual sediment extraction volumes since 1964 were roughly 50% of the sediment influx (Ham & Church, 2012). Based on a mean gravel flux of 8,800 m³/a (bulk) or 6,000 m³/a at Mission located 15 km downstream from the GST (Ham, 2005), we assume about 7,000 m³/a of the gravel flux to pass the front. This implies that the gravel flux contributing to wedge progradation, $Q_0 p_0$, is within the range 43,000–63,000 m³/a. Subsidence due to consolidation of shallow Holocene sediments in the Fraser lowlands is about 1.5 mm/a (Mazzotti et al., 2009) and the rate of sea level rise, $\xi$, in the Fraser delta in the 20th century was 1.75 mm/a (Mazzotti et al., 2009). As our model cannot deal with delta processes such as bifurcations, we simply assume the lengthening rate of the main channel, $\beta$, equal to the Fraser delta progradation rate of 2.4 m/a (Williams & Roberts, 1989). Naturally, the uncertainty of the above numbers is large, but they give a predicted long-term average value of the GST migration celerity within the range −2 to 2 m/a.

This implies no more than a ±100 m change in GST position over a 50 year period, which matches with the negligible GST advance estimated over the period 1949–1999, whereas the 600–800 m GST advance within the period 1999–2014 may be related to the increased gravel flux due to channel alignment upstream of Agassiz-Rosedale Bridge. We estimated the GST advance from aerial images from Church and Ham (2004) and Google Earth, all taken at low flows of about 700 m³/s and assuming the downstream end of the downstream gravel bar to indicate the gravel front. The main point here is that subsidence, sea level rise, and gravel overtaking the front brings the predicted celerity down to values that reasonably agree with the observations.

## 8. Conclusions

Even a limited content of gravel in the sediment supply to a sand reach results in the formation of a progradational gravel wedge with a higher slope. As slope adjusts to mainly the coarse mode in the sediment supply, a gravel-sand transition (GST) forms at the wedge front where the load runs out of gravel. The large slope in the gravel reach makes sand so mobile that a small surface sand content (typically 10–20%) suffices to transport the sand supply downstream.

The GST migrates more slowly as the length of the gravel reach increases. Subsidence, base level rise, and delta progradation lead to GST halt, provided that the stable GST position does not exceed the domain. Otherwise the entire domain eventually becomes gravel bedded. A GST can retreat due to an increased rate of subsidence, sea level rise, or delta progradation.

We present analytical formulations to estimate the GST migration celerity and the stable GST position. Combined with quasi-equilibrium closure relations for slope and surface texture, the model captures GST dynamics well. Predicted modern migration celerities for the Allt Dubhaig and Fraser River GSTs compare well with measured data.

## Appendix A: Conservation of Gravel Wedge Mass

We formulate the GST migration model based on conservation of sediment mass in the gravel wedge (Figure 2). A change in the gravel wedge volume, $\Delta V$, occurs if (1) the gravel front migrates, (2) the mean gravel reach slope $\bar{S}_u$ (with subscript $u$ indicating the gravel reach) changes, or (3) the vertical distance $h_A$ (i.e., the vertical distance between the front crest and elevation $\eta_B$ that is subject to subsidence or uplift) changes:

$$\Delta V = \Delta V_1 + \Delta V_2 + \Delta V_3 \qquad (A1)$$

where

$$\Delta V_1 = B x_A \bar{S}_u \Delta x_A \qquad (A2)$$

$$\Delta V_2 = \frac{1}{2} B x_A^2 \Delta \bar{S}_u \qquad (A3)$$

$$\Delta V_3 = B x_A \Delta h_A \qquad (A4)$$

where $B$ denotes the channel width and $x_A$ is the distance between the wedge front and the upstream boundary of the domain at $x_0$ ($x_0 = 0$). The subscripts 0 and $A$ indicate, respectively, the upstream boundary of the model domain and the position of the gravel front. In equations (A2) and (A4) we consider the sediment

volume within the extended wedge front negligible in the reach scale budget of bed material (i.e., in Figure 2 the yellow areas are neglected compared to the purple areas), which is reasonable if $x_A$ covers a significant distance.

The combination of equations (A1)–(A4) yields the time rate of change of the gravel wedge volume

$$\frac{dV}{dt} = Bx_A \bar{S}_u c_A + \frac{1}{2}Bx_A^2 \frac{d\bar{S}_u}{dt} + Bx_A \frac{dh_A}{dt} \qquad (A5)$$

where $t$ denotes time, $c_A$ the wedge front migration celerity ($c_A = dx_A/dt$), and $h_A$ is equal to (Figure 2):

$$h_A = \eta_{w\,base} - \bar{H}_u + (L - x_A)\bar{S}_d - \eta_B \qquad (A6)$$

where $\eta_{w\,base}$ denotes the base level relative to a fixed datum, $\bar{H}_u$ the mean flow depth in the gravel reach, $L$ the domain length, $\bar{S}_d$ is the mean sand reach slope (with subscript $d$ indicating the sand reach), and $\eta_B$ is an elevation relative to the fixed datum (Figure 2).

The time rate of change of sediment volume in the gravel wedge is equal to the net sediment supply to the gravel reach:

$$c_b \frac{dV}{dt} = Q_0 - Q_A \qquad (A7)$$

where $Q$ denotes the total bed material load (i.e., gravel and sand) and $c_b$ is the concentration of bed sediment ($c_b = 1 - \lambda_p$, where $\lambda_p$ denotes the porosity of bed sediment). The sediment supply, $Q_0$, may change with time and is assumed to be unaffected by GST migration.

All gravel is assumed to build the gravel reach slope and to lengthen the gravel reach, which implies that, by definition, gravel does not enter the sand reach ($Q_{gA} = 0$):

$$c_b \frac{dV_g}{dt} = Q_{g0} \qquad (A8)$$

where the subscript $g$ indicates gravel. The time rate of change of gravel volume in the wedge can also be written as

$$\frac{dV_g}{dt} = \bar{F}_W \frac{dV}{dt} \qquad (A9)$$

where $\bar{F}_W$ denotes the mean gravel content in the wedge deposit. In deriving equation (A9) we have assumed $\bar{F}_W$ to slowly change with time and have neglected the $d\bar{F}_W/dt$ term. Under aggradational conditions over the gravel reach, $\bar{F}_W$ is a weighted average of the gravel content in the load and the bed surface gravel content $\bar{F}_u$ (Hoey & Ferguson, 1994):

$$\bar{F}_W = \alpha p_0 + (1 - \alpha)\bar{F}_u \qquad (A10)$$

where $\alpha$ denotes a constant varying between 0 and 1 and $p_0$ is the gravel content in the sediment supply. Just as $Q_0$, $p_0$ may change with time and is assumed to be unaffected by GST migration. Under degradational conditions over the gravel reach, $\bar{F}_W$ is equal to the gravel content in the previously deposited wedge sediment.

The combination of equations (A7)–(A9) yields a formulation for the sand supply to the sand reach, $Q_{sA}$:

$$Q_{sA} = Q_0 \left(1 - \frac{p_0}{\bar{F}_W}\right) \qquad (A11)$$

where the subscript $s$ indicates sand. As the gravel content in the wedge deposit, $\bar{F}_W$, is typically equal or larger than the gravel content in the sediment supply $p_0$ (Hoey & Ferguson, 1994; Parker, 1991), the sand supply to the sand reach varies between 0 and the upstream sand supply, $Q_{s0}$ ($0 \leq Q_{sA} \leq Q_{s0}$). This confirms the fact that the formation of a gravel wedge reduces the sand supply to the sand reach.

## Appendix B: Details of the GST Migration Celerity

The combination of equations (A5), (A6), (A8), and (A9) yields for the GST migration celerity, $c_A$:

$$c_A = \frac{1}{\bar{S}_u - \bar{S}_d} \left[ \frac{Q_0}{c_b B} \frac{p_0}{\bar{F}_W} \frac{1}{x_A} - \xi - \bar{S}_d \beta + \omega + \frac{d\bar{H}_u}{dt} - (L - x_A) \frac{d\bar{S}_d}{dt} - \frac{1}{2} x_A \frac{d\bar{S}_u}{dt} \right] \tag{B1}$$

where $\xi$ denotes the rate of sea level rise ($\xi = d\eta_{w\,base}/dt$), $\beta$ the delta progradation rate ($\beta = dL/dt$), and $\omega$ is the uplift rate ($\omega = d\eta_B/dt$). Assuming the temporal change of the gravel reach slope and flow depth, and the sand reach slope to generally be small, equation (B1) can be simplified to

$$c_A = \frac{1}{\bar{S}_u - \bar{S}_d} \left[ \frac{Q_0}{c_b B} \frac{p_0}{\bar{F}_W} \frac{1}{x_A} - \xi - \bar{S}_d \beta + \omega \right] \tag{B2}$$

In the absence of subsidence, uplift, delta progradation, and base level change, separation of variables yields the GST migration celerity and GST position as a function of time:

$$c_A = \sqrt{\frac{m}{2t}}, \qquad x_A = \sqrt{2mt}, \qquad m = \frac{1}{\bar{S}_u - \bar{S}_d} \frac{Q_0}{c_b B} \frac{p_0}{\bar{F}_W} \tag{B3}$$

as well as the time $t_A$ required for a GST to travel a distance $x_A$ as a result of a limited gravel content in the sediment supply to a sand reach:

$$t_A = \frac{c_b}{2} \frac{(\bar{S}_u - \bar{S}_d) B}{Q_0} \frac{\bar{F}_W}{p_0} x_A{}^2 \tag{B4}$$

which is of similar form as the half time of bed elevation change under base level fall and unisize sediment conditions (De Vries, 1975, 1993).

For $x_A = 0$ the analytical formulation for the GST migration celerity tends to infinity. This is because the wedge volume is zero and any change to it is infinitely large. It implies that the model is not suited to describe the GST migration celerity for small values of $x_A$.

## Appendix C: Specifications of Validation

The backwater-Hirano model runs are made using the one-dimensional numerical research code Elv (Blom et al., 2017). The time step is 2 days and the spatial step is 500 m. The active layer thickness and the vertical grid cell size for keeping track of the substrate texture are equal to 1 m. The depositional flux to the substrate is defined according to equation (A10) with $\alpha = 0.3$. The domain length is 200 km.

In applying the extended model we use the same values for the time step, $\alpha$, and domain length. We integrate the GST migration celerity over time using a first-order explicit Euler scheme to compute the GST position, $x_A$, at time $t$. The initial GST position, $x_A(t_0)$, is set equal to 250 m (with $t_0 = 50$ a) to avoid the GST migration celerity from being equal to infinity at $t = 0$.

The two models are applied to a base case with gravel and sand sizes equal to 16 mm and 0.6 mm. The nondimensional friction coefficient, $C_f$, is 0.004, the porosity of the bed sediment is 0.35, and the mass densities of water and sediment are 1,000 kg/m³ and 2,650 kg/m³, respectively. We apply the Ashida and Michiue (1972) load relation, which accounts for grain size selective transport, a threshold for significant transport, and hiding. Rates of base level change, subsidence, uplift, and delta progradation are equal to zero. The water discharge per unit width is 2 m²/s and the sediment supply rate per unit width is $0.4 \cdot 10^{-4}$ m²/s. The sediment supply consists of 30% gravel, yet the initial conditions correspond to an equilibrium reach where the sediment supply consists of 100% sand. Case 2 differs from the base case regarding a decrease in the gravel and sand supply by 50% over a period of 50 years after 500 years. Cases 3a–3e are equal to the base case, apart from rates of base level rise, $\xi$, of, respectively, 4, 6, 7.5, 10, and 12 mm/a and a domain length of 300 km.

For the base case both models predict slopes in the gravel reach and sand reach equal to, respectively, about $7.5 \cdot 10^{-4}$ and $5 \cdot 10^{-5}$, and the predicted bed surface gravel content in the gravel reach is about 0.78. In the supply reduction case (Case 2) the small peaks in the GST migration celerity (Figure 3a) are associated with the quasi-equilibrium assumption of the extended model: the slopes of the two reaches adjust too quickly to the changing conditions.

# References

Ashida, K., & Michiue, M. (1972). Study on hydraulic resistance and bed-load transport rate in alluvial streams. *Transactions Japan Society of Civil Engineering*, *206*, 59–69.

Baumanis, C., & Kim, W. (2016). Reverse migration of lithofacies boundaries and shoreline in response to sea-level rise. *Basin Research*, 1–12. https://doi.org/10.1111/bre.12209

Blom, A., Arkesteijn, L., Chavarrías, V., & Viparelli, E. (2017). The equilibrium alluvial river under variable flow and its channel-forming discharge. *Journal of Geophysical Research: Earth Surface*, *122*. https://doi.org/10.1002/2017JF004213

Blom, A., Viparelli, E., & Chavarrías, V. (2016). The graded alluvial river: Profile concavity and downstream fining. *Geophysical Research Letters*, *43*, 1–9. https://doi.org/10.1002/2016GL068898

Church, M. (2006). Bed material transport and the morphology of alluvial river channels. *Annual Review of Earth and Planetary Sciences*, *34*, 325–354. https://doi.org/10.1146/annurev.earth.33.092203.122721

Church, M., & Ham, D. (2004). Atlas of the alluvial gravel-bed reach of Fraser River in the Lower Mainland. Tech. Rep. Vancouver, BC: Univ. of British Columbia.

De Vries, M. (1975). A morphological time-scale for rivers. In *Proceedings of 16th International Association for Hydraulic Research World Congress*. São Paulo, Brazil, 147, Delft Hydraulics Laboratory, Netherlands.

De Vries, M. (1993). *Use of Models for River Problems*, (p. 85). UNESCO: Paris.

Dingle, E. H., Attal, M., & Sinclair, H. D. (2017). Abrasion-set limits on Himalayan gravel flux. *Nature*, *544*, 471–474. https://doi.org/10.1038/nature22039

Dong, T. Y., Nittrouer, J. A., Il'icheva, E., Pavlov, M., McElroy, B., Czapiga, M. J., . . . Parker, G. (2016). Controls on gravel termination in seven distributary channels of the Selenga River Delta, Baikal Rift basin, Russia. *Geological Society of America Bulletin*, *128*(7-8), 1297–1312. https://doi.org/10.1130/B31427.1

Ferguson, R. I. (2003). Emergence of abrupt gravel to sand transitions along rivers through sorting processes. *Geology*, *31*(2), 159–162. https://doi.org/10.1130/0091-7613(2003)031<0159:EOAGTS>2.0.CO;2

Ferguson, R. I., Bloomer, D. J., & Church, M. (2011). Evolution of an advancing gravel front: Observations from Vedder Canal, British Columbia. *Earth Surface Processes and Landforms*, *36*(9), 1172–1182. https://doi.org/10.1002/esp.2142

Ferguson, R., Hoey, T., Wathen S., & Werritty, A. (1996). Field evidence for rapid downstream fining of river gravels through selective transport. *Geology*, *24*(2), 179–182. https://doi.org/10.1130/0091-7613(1996)024<0179:FEFRDF>2.3.CO;2

Ferguson, R. I., Hoey, T. B., Wathen, S. J., Werritty, A., Hardwick, R. I., & Sambrook Smith, G. H. (1998). Downstream fining of river gravels: Integrated field, laboratory and modeling study. In P. C. Klingeman et al. (Eds.), *Gravel-Bed Rivers in the Environment* (pp. 85–114). Highlands Ranch, CO: Water Resources Publications LLC.

Ham, D. G. (2005). *Morphodynamics and Sediment Transport in a Wandering Gravel-Bed Channel: Fraser River, British Columbia*, (PhD thesis). Vancouver, BC: Univ. of British Columbia.

Ham, D., & Church, M. (2012). Morphodynamics of an extended bar complex, Fraser River, British Columbia. *Earth Surface Processes and Landforms*, *37*(10), 1074–1089. https://doi.org/10.1002/esp.3231

Hirano, M. (1971). River bed degradation with armoring. *Transactions Japan Society of Civil Engineers*, *3*(2), 194–195.

Hoey, T. B., & Ferguson, R. (1994). Numerical simulation of downstream fining by selective transport in gravel bed rivers: Model development and illustration. *Water Resources Research*, *30*(7), 2251–2260. https://doi.org/10.1029/94WR00556

Howard, A. D. (1980). Thresholds in river regimes. In D. R. Coates and J. D. Vitek (Eds.), *Thresholds in Geomorphology* (pp. 227–258). Boston: Allen and Unwin.

Howard, A. D. (1982). Equilibrium and time scales in geomorphology: Application to sand-bed alluvial streams. *Earth Surface Processes and Landforms*, *7*(4), 303–325. https://doi.org/10.1002/esp.3290070403

Jerolmack, D. J., & Brzinski, T. A. (2010). Equivalence of abrupt grain-size transitions in alluvial rivers and eolian sand seas: A hypothesis. *Geology*, *38*(8), 719–722. https://doi.org/10.1130/G30922.1

Lamb, M. P., & Venditti, J. G. (2016). The grain size gap and abrupt gravel-sand transitions in rivers due to suspension fallout. *Geophysical Research Letters*, *43*(8), 3777–3785. https://doi.org/10.1002/2016GL068713

Leopold, L. (1992). Sediment size that determines channel morphology. In P. Billi et al. (Eds.), *Dynamics of Gravel-Bed Rivers* (pp. 297–311). New York: John Wiley Ltd.

Litwin Miller, K., Reitz, M. D., & Jerolmack, D. J. (2014). Generalized sorting profile of alluvial fans. *Geophysical Research Letters*, *41*, 7191–7199. https://doi.org/10.1002/2014GL060991

Mackin, J. H. (1948). Concept of the graded river. *Geological Society of America Bulletin*, *59*(5), 463–512. https://doi.org/10.1130/0016-7606(1948)59

Marr, J. G., Swenson, J. B., Paola, C., & Voller, V. R. (2000). A two-diffusion model of fluvial stratigraphy in closed depositional basins. *Basin Research*, *12*(3–4), 381–398. https://doi.org/10.1111/j.1365-2117.2000.00134.x

Mazzotti, S., Lambert, A., Van der Kooij, M., & Mainville, A. (2009). Impact of anthropogenic subsidence on relative sea-level rise in the Fraser River delta. *Geology*, *37*(9), 771–774. https://doi.org/10.1130/G25640A.1

McLean, D. G., Church, M., & Tassone, B. (1999). Sediment transport along lower Fraser River: 1. Measurements and hydraulic computations. *Water Resources Research*, *35*(8), 2533–2548. https://doi.org/10.1029/1999WR900101

Paola, C. (2001). Modelling stream braiding over a range of scales. In M. P. Mosley (Ed.), *Gravel-Bed Rivers V* (pp. 11–46). Wellington: New Zealand Hydrological Society.

Paola, C., & Leeder, M. (2011). Environmental dynamics: Simplicity versus complexity. *Nature*, *469*, 38–39. https://doi.org/10.1038/469038a

Paola, C., Heller, P. L., & Angevine, C. L. (1992). The large-scale dynamics of grain-size variation in alluvial basins, 1: Theory. *Basin Research*, *4*(2), 73–90. https://doi.org/10.1111/j.1365-2117.1992.tb00145.x

Paola, C., Parker, G., Seal, R., Sinha, S. K., Southard, J. B., & Wilcock, P. R. (1992). Downstream fining by selective deposition in a laboratory flume. *Science*, *258*(5089), 1757–1760. https://doi.org/10.1126/science.258.5089.1757

Parker, G. (1991). Selective sorting and abrasion of river gravel. I: Theory. *Journal of Hydraulic Engineering*, *117*(2), 131–147. https://doi.org/10.1061/(ASCE)0733-9429(1991)117:2(131)

Parker, G. (2004). Morphodynamics of gravel-sand transitions, Chap. 27, In *1D sediment transport morphodynamics with applications to rivers and turbidity currents*, E-Book. [Available at: http://hydrolab.illinois.edu/people/parkerg/morphodynamics_e-book.htm.]

Parker, G., & Cui, Y. (1998). The arrested gravel front: Stable gravel-sand transitions in rivers. Part 1: Simplified analytical solution. *Journal of Hydraulic Research*, *36*(1), 75–100. https://doi.org/10.1080/00221689809498379

Parker, G., Klingeman, P. C., & McLean, D. G. (1982). Bedload and size distribution in paved gravel-bed streams. *Journal of the Hydraulics Division*, *108*(4), 544–571.

Sambrook Smith, G. H., & Ferguson, R. I. (1995). The gravel-sand transition along river channels. *Journal of Sedimentary Research*, *65*(2A), 423–430. https://doi.org/10.1306/D42680E0-2B26-11D7-8648000102C1865D

Shaw, J., & Kellerhals, R. (1982). The composition of recent alluvial gravels in Alberta river beds. *Alberta Research Council Bulletin*, *41*, p. 151.

Sinha, S. K., & Parker, G. (1996). Causes of concavity in longitudinal profiles of rivers. *Water Resources Research*, *32*(5), 1417–1428. https://doi.org/10.1029/95WR03819

Sternberg, H. (1875). Untersuchungen über Längen- und Querprofil geschiebeführender Flüsse. *Zeitschrift für Bauwesen*, *25*, 483–506.

Venditti, J. G., & Church, M. (2014). Morphology and controls on the position of a gravel-sand transition: Fraser River, British Columbia. *Journal of Geophysical Research: Earth Surface*, *119*, 1959–1976. https://doi.org/10.1002/2014JF003147

Venditti, J. G., Domarad, N., Church, M., & Rennie, C. D. (2015). The gravel-sand transition: Sediment dynamics in a diffuse extension. *Journal of Geophysical Research: Earth Surface*, *120*(6), 943–963. https://doi.org/10.1002/2014JF003328

Wathen, S. J., Ferguson, R. I., Hoey, T. B., & Werritty, A. (1995). Unequal mobility of gravel and sand in weakly bimodal river sediments. *Water Resources Research*, *31*(8), 2087–2096. https://doi.org/10.1029/95WR01229

Wilcock, P. R. (1998). Two-fraction model of initial sediment motion in gravel-bed rivers. *Science*, *280*(5362), 410–412. https://doi.org/10.1126/science.280.5362.410

Wilcock, P. R., & Crowe, J. C. (2003). Surface-based transport model for mixed-size sediment. *Journal of Hydraulic Engineering*, *129*(2), 120–128. https://doi.org/10.1061/(ASCE)0733-9429(2003)129:2(120)

Williams, H. F. L., & Roberts, M. C. (1989). Holocene sea-level change and delta growth: Fraser River delta, British Columbia. *Canadian Journal of Earth Sciences*, *26*(9), 1657–1666. https://doi.org/10.1139/e89-142

Wolcott, J. (1988). Nonfluvial control of bimodal grain-size distributions in river-bed gravels. *Journal of Sedimentary Research*, *58*(6), 979–984. https://doi.org/10.1306/212F8ED6-2B24-11D7-8648000102C1865D

Yatsu, E. (1955). On the longitudinal profile of the graded river. *Eos, Transactions American Geophysical Union*, *36*(4), 655–663. https://doi.org/10.1029/TR036i004p00655